

Bidirectionally tuning Kapitza conductance through the inclusion of substitutional impurities

John C. Duda, Timothy S. English, Edward S. Piekos, Thomas E. Beechem, Thomas W. Kenny et al.

Citation: *J. Appl. Phys.* **112**, 073519 (2012); doi: 10.1063/1.4757941

View online: <http://dx.doi.org/10.1063/1.4757941>

View Table of Contents: <http://jap.aip.org/resource/1/JAPIAU/v112/i7>

Published by the [American Institute of Physics](#).

Related Articles

Role of ethylene on surface oxidation of TiO₂(110)

Appl. Phys. Lett. **101**, 211601 (2012)

Communication: An obligatory glass surface

J. Chem. Phys. **137**, 141102 (2012)

Pressure dependency of thermal boundary conductance of carbon nanotube/silicon interface: A molecular dynamics study

J. Appl. Phys. **112**, 053501 (2012)

Effect of nanopatterns on Kapitza resistance at a water-gold interface during boiling: A molecular dynamics study

J. Appl. Phys. **112**, 053508 (2012)

Phononic dispersion of a two-dimensional chessboard-patterned bicomponent array on a substrate

Appl. Phys. Lett. **101**, 053102 (2012)

Additional information on J. Appl. Phys.

Journal Homepage: <http://jap.aip.org/>

Journal Information: http://jap.aip.org/about/about_the_journal

Top downloads: http://jap.aip.org/features/most_downloaded

Information for Authors: <http://jap.aip.org/authors>

ADVERTISEMENT



AIP Advances

Now Indexed in Thomson Reuters Databases

Explore AIP's open access journal:

- Rapid publication
- Article-level metrics
- Post-publication rating and commenting

Bidirectionally tuning Kapitza conductance through the inclusion of substitutional impurities

John C. Duda,^{1,2,a)} Timothy S. English,^{3,2} Edward S. Piekos,² Thomas E. Beechem,² Thomas W. Kenny,³ and Patrick E. Hopkins^{1,b)}

¹*Department of Mechanical and Aerospace Engineering, University of Virginia, Charlottesville, Virginia 22904, USA*

²*Sandia National Laboratories, Albuquerque, New Mexico 87185, USA*

³*Department of Mechanical Engineering, Stanford University, Stanford, California 94305, USA*

(Received 21 May 2012; accepted 10 September 2012; published online 10 October 2012)

We investigate the influence of substitutional impurities on Kapitza conductance at coherent interfaces via non-equilibrium molecular dynamics simulations. The reference interface is comprised of two mass-mismatched Lennard-Jones solids with atomic masses of 40 and 120 amu. Substitutional impurity atoms with varying characteristics, e.g., mass or bond, are arranged about the interface in Gaussian distributions. When the masses of impurities fall outside the atomic masses of the reference materials, substitutional impurities impede interfacial thermal transport; on the other hand, when the impurity masses fall within this range, impurities enhance transport. Local phonon density of states calculations indicate that this observed enhancement can be attributed to a spatial grading of vibrational properties near the interface. Finally, for the range of parameters investigated, we find that the mass of the impurity atoms plays a dominant role as compared to the impurity bond characteristics. © 2012 American Institute of Physics. [<http://dx.doi.org/10.1063/1.4757941>]

I. INTRODUCTION

In semiconductor materials, phonon mean-free-paths can exceed several hundred nanometers.^{1,2} In systems where the distance between interfaces is on the order of or less than this length scale, thermal transport properties are dictated as much by the interfaces between materials as they are by the materials themselves.^{3,4} The efficiency of thermal transport across a solid-solid interface can be described by the interface Kapitza conductance⁵ or h_K . At a near-ideal interface, i.e., free of defects and compositionally abrupt, Kapitza conductance is inherently limited by the overlap of the phonon spectra of the two solids comprising the interface.^{6–11} That is, the better matched the vibrational spectra of the materials, the higher the Kapitza conductance. However, other qualities of the interface can influence Kapitza conductance, including interfacial structure,^{12–22} interfacial chemistry,^{23–30} and the relative orientation of the constituent materials.^{12,31–35}

With regard to interface structure, deviations from “ideality” can include one or a combination of several unique features, e.g., compositional mixing,^{9,22} dislocations,¹⁶ confined films,^{21,22} non-crystallinity,¹³ or nanometer-scale geometric facets.^{15,18–20} When compared to ideal interfaces, certain combinations of these features have been found to enhance Kapitza conductance,^{9,21,22} while others have been shown to reduce it.^{9,13,15,16,18,19} A subset of these studies have demonstrated that careful control over interfacial structure can provide a means of tuning Kapitza conductance.^{17–22} More specifically, the results of Refs. 17–19 have shown that nanometer-scale geometric facets achieved through quantum-

dot patterning^{17,18} or chemical etching¹⁹ can lead to lower realized values of Kapitza conductance as compared to that at nominally flat (compositionally sharp) interfaces. On the other hand, Refs. 20–22 have indicated that careful control over interfacial structure either through nano-patterning²⁰ or the inclusion of a confined thin film^{21,22} can enhance conductance by way of grading vibrational properties.

In this report, we investigate the influence of substitutional impurities on Kapitza conductance at coherent interfaces via non-equilibrium molecular dynamics (NEMD) simulations. It is shown that the inclusion of impurities in the vicinity of the interface can provide a means of bidirectionally tuning Kapitza conductance. The reference interface is comprised of two mass-mismatched Lennard-Jones solids, with masses m_A and m_B , and impurities of mass m_i are arranged symmetrically about the interface in a Gaussian distribution. When $m_i < m_A$ or $m_i > m_B$, Kapitza conductance is lower than that at the reference interface, whereas when $m_A < m_i < m_B$, conductance is higher. This is contrary to the concept of phonon-impurity scattering in the context of thermal conductivity, where the scattering rate (inverse of scattering time) is often described in a form $\tau_i^{-1} \propto ((m_{host} - m_i)/m_{host})^2$, and impurities always impede thermal transport.^{36,37} As in previous work investigating the thermal conductivity of alloys,³⁸ we find that the mass of the impurity atoms plays a dominant role as compared to the impurity bond characteristics (strength or radius).

II. COMPUTATIONAL DETAILS

All computational cells were $8 \times 8 \times 80$ face centered cubic conventional unit cells in size and contained 20480 atoms such that size effects were mitigated;^{28,35} one half of the atoms were A-type and the other half were B-type,

^{a)}Electronic mail: duda@virginia.edu.

^{b)}Electronic mail: phopkins@virginia.edu.

TABLE I. The maximum impurity concentration (η), distribution full-width half-max (FWHM), number of impurities (n_i), impurity atom mass (m_i), impurity atom length parameter (σ_i), impurity atom energy parameter (ε_i), and mean and standard deviations of Kapitza conductances at 30 K (h_K and Σ_h , respectively). Standard deviations increased slightly with increasing simulation temperature and were near to zero at low temperatures.

	Sample	η (%)	FWHM (nm)	n_i	m_i (amu)	σ_i (\AA)	ε_i (eV)	h_K at 30 K ($\text{W m}^{-2}\text{K}^{-1}$)	Σ_h at 30 K ($\text{W m}^{-2}\text{K}^{-1}$)
Baseline	A	0						97.7	6.4
Distribution series	B	10	10	54	10	3.37	0.0103	76.9	11.0
	C	20	10	102	10	3.37	0.0103	64.1	3.7
	D	40	10	206	10	3.37	0.0103	51.8	4.3
	E	20	20	213	10	3.37	0.0103	54.6	3.6
Mass series	B	10	10	54	10	3.37	0.0103	76.9	11.0
	F	10	10	54	80	3.37	0.0103	107.0	15.2
	G	10	10	54	150	3.37	0.0103	82.7	8.5
Bond series	H	20	10	102	10	3.37	0.0077	65.7	4.1
	C	20	10	102	10	3.37	0.0103	64.1	3.7
	I	20	10	102	10	3.37	0.0129	61.0	2.5

separated by an interface at the midpoint of the computational cell in the z -direction. All interactions were described by the 6–12 LJ potential, $U(r) = 4\varepsilon[(\sigma/r)^{12} - (\sigma/r)^6]$, where r is the interatomic separation and σ and ε are the LJ length and energy parameters; the potential was parameterized for Ar,³⁹ where $\sigma = 3.37 \text{ \AA}$ and $\varepsilon = 0.0103 \text{ eV}$ (except for those simulations discussed in Sec. III C where impurity bond characteristics were altered). The cutoff distance (radius beyond which the potential was truncated and $U=0$) was set to $r_c = 2.5\sigma$. A- and B-type atoms were distinguished by their masses alone; $m_A = 40 \text{ amu}$ and $m_B = 120 \text{ amu}$. Substitutional impurities of varying m_i , ε_i , or σ_i were then arranged symmetrically about the interface in a Gaussian distribution. To do so, we assigned each atom a random value between 0 and 1; if the numeric value was less than the desired concentration of impurities at the atom's spatial coordinate, it was treated as an impurity atom. To ensure that a particular arrangement of impurities did not impact our results, different domains were constructed with the same concentration profile but with different absolute distributions; no statistically significant differences in calculated Kapitza conductances were noted. The specifics of each domain are listed in Table I.

Periodic boundary conditions were applied in the x - and y -directions and the four outermost monolayers in the positive and negative z -directions formed rigid walls. The eight monolayers immediately inside these walls were bath atoms, to which energy would be added or removed to establish a temperature gradient. During the simulation, the equations of motion for the system were integrated using the Nordsieck fifth-order predictor corrector algorithm⁴⁰ with a time step of 4.28 fs. The systems were equilibrated at a predefined temperature via a velocity scaling routine and zero pressure, maintained by the Berendsen barostat algorithm.⁴¹ Once equilibration was complete, velocity-fluctuation time series were generated for computation of the local phonon density of states (DOS). Subsequently, the NEMD procedure was implemented. The addition of energy to/removal from the baths was performed through a constant-flux approach;^{35,42,43} the flux, Q , was set to 0.54 MW m^{-2} . During NEMD, the systems

were divided into 160 equally sized bins such that spatial temperature profiles could be calculated along the z -axis. Once in steady-state, time-averaged profiles were constructed from 4000 system snapshots taken over 2×10^6 time steps (8.56 ns). A linear least-squares fit was then performed for each half of the domain. The five bins nearest to the bath and the interface were not included in these fits. The discontinuity between the fits at the interface, ΔT , was used to calculate h_K through the relationship $Q = h_K \Delta T$.

III. RESULTS AND DISCUSSION

The Kapitza conductance at the reference interface (sample A) is plotted as a function of temperature in both Figs. 1 and 2 (black squares) and the dashed lines are linear fits of the data. Each data point represents the mean result of five independent simulations and error bars represent the standard deviation of this average, i.e., repeatability. The

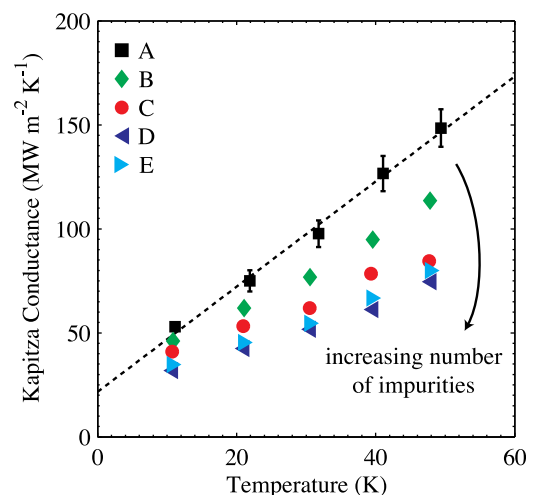


FIG. 1. The effects of the concentration and distribution of light impurities, $m_i = 10 \text{ amu}$, on Kapitza conductance as a function of temperature, where the conductance at the reference interface (sample A) is represented by the squares, and the dotted line is a linear fit of the data. The data indicate that doubling the number of impurities does not double the realized reduction in Kapitza conductance (comparing B, C, and D).

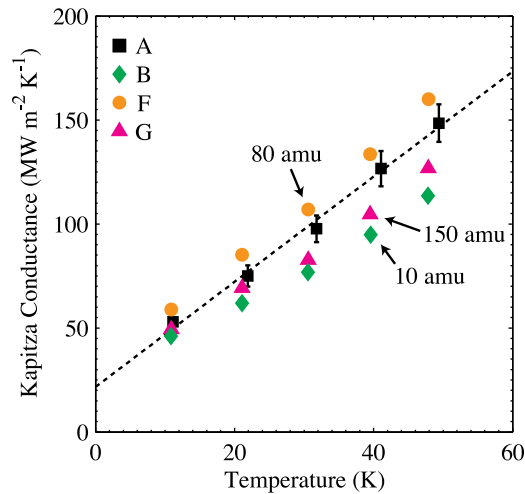


FIG. 2. The effect of variable impurity mass on Kapitza conductance as a function of temperature. When m_i falls outside the range between m_A and m_B , Kapitza conductances are lower than that at the reference interface, while conductances increase when m_i falls between m_A and m_B .

standard deviation increases with increasing temperature due to the fact that our calculations are less sensitive to Kapitza conductance with increasing temperature (the temperature drop at the interface associated with Kapitza conductance decreases, while the temperature drops across the leads increases). Kapitza conductances at the interfaces contained within samples B through G (impurity distribution and mass series) were calculated as a function of temperature from 11 K to 50 K, and the conductances at the interfaces in samples H and I (bond series) were calculated at a fixed temperature of 30 K.

A. Influence of impurity distribution

The effects of the concentration and distribution of light impurities ($m_i = 10$ amu) are shown in Fig. 1. When comparing the results from samples B, C, and D, it is clear that Kapitza conductance decreases with increasing impurity concentration; as in earlier works, increased interfacial disorder leads to lower realized values of Kapitza conductance, as well as a diminished temperature dependence.^{9,13,15,16,18,19} However, these data also show that the relationship between impurity concentration and the effective reduction in Kapitza conductance is non-linear; that is, doubling the number of impurities does not double the realized reduction in Kapitza conductance, which can be seen by comparing the difference in Kapitza conductance between B and C to the difference between C and D. This is consistent with the behavior observed in SiGe alloys, where increasing Ge concentration had a diminishing effect in terms of yielding lower values of thermal conductivity.^{44,45} However, in our earlier work in which substrates were chemically etched to vary interface roughness (i.e., interface disorder) we observed the opposite behavior, where relative reductions in Kapitza conductance increased with increasing disorder.¹⁹ Thus, taken collectively, these works serve to distinguish the effects of compositional and structural disorder. While both can be exploited to tune interfacial transport, the behavior of each is distinct.

B. Influence of impurity mass

The effect of impurity mass for a fixed distribution is shown in Fig. 2. Both light and heavy impurities (samples B and G, or $m_i = 10$ amu and 150 amu, respectively) reduce conductance from the baseline values, albeit this reduction is not symmetric with impurity mass. Conventional forms of the phonon-impurity scattering rate are of the form $\tau_i^{-1} \propto ((m_{\text{host}} - m_i)/m_{\text{host}})^2$. Thus, in a medium where the average atomic mass is 80 amu, 10 amu, and 150 amu impurities would behave identically.^{36,37} While this form of phonon scattering can hold in the context of thermal conductivity, the fact that it does not hold at an interface suggests other mechanisms are, in part, responsible for the observed behavior. Also shown in Fig. 2 is that when m_i falls between m_A and m_B (sample F, or $m_i = 80$ amu), conductance increases, or, in other words, increased interfacial disorder increases the efficiency of thermal transport.

To further explore the mechanisms responsible for this observed behavior, we have calculated the local phonon DOS of each atom within the monolayers immediately adjacent to the interface. The DOS is proportional to the Fourier transform (\mathcal{F}) of the velocity auto-correlation function (VACF)⁴⁰ but in practice is calculated using standard estimation procedures for power spectral density. For each atom, the velocity is obtained at each integration time step to give a velocity fluctuation time series of 73 728 points. The Welch method of power spectral density estimation is then applied by creating eight 50% overlapping segments of 16 384 points to give an angular frequency resolution of $8.96 \times 10^{10} \text{ rad s}^{-1}$ based on our time step of 4.28 fs. Each segment is then multiplied by a Hamming window and the fast Fourier transform is computed. The power spectral density, equivalent to $\mathcal{F}(\text{VACF})$, is then obtained by ensemble averaging the Fourier transform magnitudes of each segment. In order to compute the DOS in units of counts per frequency per volume, $\mathcal{F}(\text{VACF})$ must be further normalized by the atomic mass, local temperature, and atomic density.²⁸

The phonon density of states of materials A and B, as well as those of 10, 80, and 150 amu impurities immediately adjacent to the interface (in samples B, F, and G, respectively) calculated at 11 K are plotted in Fig. 3(a). The primary spectral overlap between A and B falls between 5 and 7 Trad s^{-1} . While both the 80 and 150 amu impurities exhibit spectral overlap within this range, the vibrational spectrum of the 10 amu impurity is largely outside the spectra of both materials A and B, thus providing insight as to why the 10 amu impurities produce lower realized values of Kapitza conductance as compared to 150 amu impurities. Again, according to Klemens theory,^{36,37} the strength of impurity scattering is proportional $((m_{\text{host}} - m_i)/m_{\text{host}})^2$, which would suggest that the effects of 10 amu and 150 amu impurities should be the same. However, at an interface, where phonon scattering is not only dictated by a difference in absolute mass but also the overlap of phonon spectra, this does not hold. To further illustrate this point, we define the spectral overlap²⁹ between material A, an impurity atom, and material B as

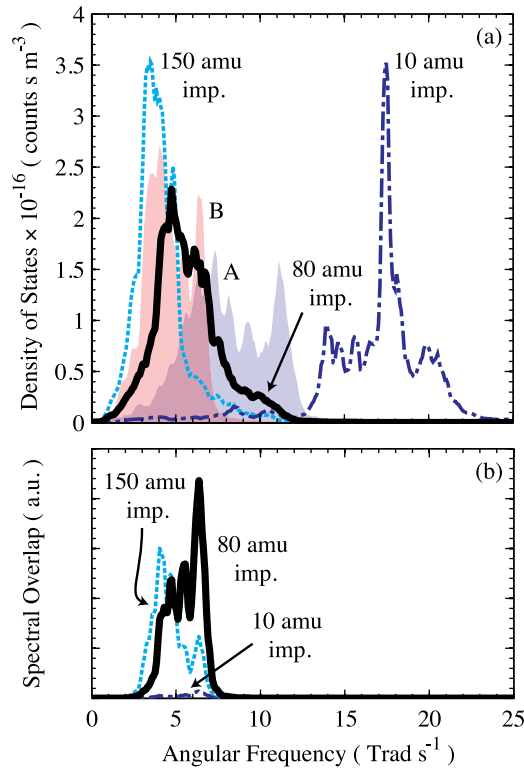


FIG. 3. The phonon density of states of materials A and B (shaded regions), as well as that of 10, 80, and 150 amu impurities immediately adjacent to the interface in samples B, F, and G (dotted, solid, and dotted-dashed lines, respectively) are shown in (a). The primary spectral overlap between A and B falls between 5 and 7 Trads^{-1} . While both the 80 and 150 amu impurities exhibit some spectral overlap within this range, the vibrational spectrum of the 10 amu impurity is largely outside the spectra of both materials A and B. In (b), the spectral overlap as defined by Eq. (1) is plotted for the three different combinations of $A:i:B$.

$$I_{A:i:B}(\omega) = D_A(\omega)D_i(\omega)D_B(\omega), \quad (1)$$

where $D_i(\omega)$ is the density of states of one of the three impurity atoms; this spectral overlap is plotted in Fig. 3(b). As is evident in the figure, while the overlap “width” of the 80 and the 150 amu impurities is similar, the area under the curve associated with the 80 amu impurity is larger (by $\approx 30\%$). In addition, the $A:80\text{ amu}:B$ overlap is centered about the inherent vibrational overlap between materials A and B, thus indicating that the 80 amu impurities can serve to act as a “vibrational bridge” by creating a region of graded vibrational properties near the interface. However, this result is unique compared to earlier work in which a confined thin film at the interface served to grade the vibrational properties insofar as impurities enhance conductance at elevated temperatures, whereas the confined films only enhanced conductance at low temperatures ($\approx 10\%$ of the melt temperature, which in the present system is $< 10\text{ K}$).²²

C. Influence of impurity bond

Impurity atoms can differ not only in terms of atomic mass but also in terms of their bond characteristics, e.g., strength and radius. In a Lennard-Jones system, these characteristics are dictated by the energy and length parameters, ϵ and σ . In a dislocation free system, a change in either ϵ or σ

will have a similar effect insofar as it will change the interatomic force constant, $K = \partial^2 U / \partial r^2$. Thus, in order to assess the influence of the impurity bond characteristics, we chose to vary the Lennard-Jones energy parameter of 10 amu impurities, ϵ_i , by $\pm 25\%$, while leaving σ fixed (by keeping bond radius fixed, the coherent nature of the interfaces could be preserved). Lorentz-Berthelot mixing rules were applied for interactions between impurity and host atoms, $\epsilon_{ij} = \sqrt{\epsilon_i \epsilon_j}$, and Kapitza conductance was calculated at a fixed temperature of 30 K. As noted in Table I, changing ϵ_i by as much as $\pm 25\%$ led to no statistically significant change in Kapitza conductance, indicating for this combination of parameters, the mass of the impurity atoms plays the dominant role as compared to the impurity bond characteristics. This is consistent with earlier molecular dynamics studies of the thermal conductivity of SiGe alloys, where treating Ge atoms like heavy Si isotopes (ignoring differences in bond strength) did not distort results.³⁸

IV. CONCLUSION

In summary, we have investigated the influence of substitutional impurities on Kapitza conductance at coherent type interfaces via non-equilibrium molecular dynamics simulations. It has been shown that the presence of impurities at an interface can either increase or reduce the Kapitza conductance at an interface depending on the relative match or mismatch between the vibrational spectra of the materials comprising the interface and that of the impurities. These results suggest that at solid-solid interfaces between lattice-matched materials, e.g., AlAs:GaAs, compositional diffusivity (disorder) via either doping or alloying could enhance thermal transport.

ACKNOWLEDGMENTS

J.C.D. and P.E.H. acknowledge funding from the National Science Foundation (CBET-1134311). T.S.E. is appreciative for funding from the National Science Foundation through the Graduate Research Fellowship Program and from the Department of Defense through the National Defense Science & Engineering Graduate Fellowship Program. This work was funded in part by the LDRD program office at Sandia National Laboratories. Sandia National Laboratories is a multiprogram laboratory managed and operated by Sandia Corporation, a wholly owned subsidiary of Lockheed Martin Corporation, for the United States Department of Energy’s National Nuclear Security Administration under Contract DE-AC04-94AL85000.

¹A. S. Henry and G. Chen, *J. Comput. Theor. Nanosci.* **5**, 141 (2008).

²D. P. Sellan, E. S. Landry, J. E. Turney, A. J. H. McGaughey, and C. H. Amon, *Phys. Rev. B* **81**, 214305 (2010).

³D. G. Cahill, W. K. Ford, K. E. Goodson, G. D. Mahan, A. Majumdar, H. J. Maris, R. Merlin, and S. R. Phillpot, *J. Appl. Phys.* **93**, 793 (2003).

⁴E. Pop, S. Sinha, and K. E. Goodson, *Proc. IEEE* **94**, 1587 (2006).

⁵P. L. Kapitza, *Phys. Rev.* **60**, 354 (1941).

⁶E. T. Swartz and R. O. Pohl, *Rev. Mod. Phys.* **61**, 605 (1989).

⁷R. J. Stoner and H. J. Maris, *Phys. Rev. B* **48**, 16373 (1993).

⁸R. J. Stevens, A. N. Smith, and P. M. Norris, *J. Heat Transfer* **127**, 315 (2005).

- ⁹R. J. Stevens, L. V. Zhigilei, and P. M. Norris, *Int. J. Heat Mass Transfer* **50**, 3977 (2007).
- ¹⁰P. E. Hopkins, P. M. Norris, and R. J. Stevens, *J. Heat Transfer* **130**, 022401 (2008).
- ¹¹P. M. Norris and P. E. Hopkins, *J. Heat Transfer* **131**, 043207 (2009).
- ¹²R. M. Costescu, M. A. Wall, and D. G. Cahill, *Phys. Rev. B* **67**, 054302 (2003).
- ¹³P. E. Hopkins, P. M. Norris, R. J. Stevens, T. E. Beechem, and S. Graham, *J. Heat Transfer* **130**, 062402 (2008).
- ¹⁴Y. Xu, R. Kato, and M. Goto, *J. Appl. Phys.* **108**, 104317 (2010).
- ¹⁵P. E. Hopkins, L. M. Phinney, J. R. Serrano, and T. E. Beechem, *Phys. Rev. B* **82**, 085307 (2010).
- ¹⁶P. E. Hopkins, J. C. Duda, S. P. Clark, C. P. Hains, T. J. Rotter, L. M. Phinney, and G. Balakrishnan, *Appl. Phys. Lett.* **98**, 161913 (2011).
- ¹⁷G. Pernot, M. Stoffel, I. Savic, F. Pezzoli, P. Chen, G. Savelli, A. Jacquot, J. Schumann, U. Denker, I. Mönch, C. Deneke, O. G. Schmidt, J. M. Rampnoux, S. Wang, M. Plissonnier, A. Rastelli, S. Dilhaire, and N. Mingo, *Nat. Mater.* **9**, 491 (2010).
- ¹⁸P. E. Hopkins, J. C. Duda, C. W. Petz, and J. A. Floro, *Phys. Rev. B* **84**, 035438 (2011).
- ¹⁹J. C. Duda and P. E. Hopkins, *Appl. Phys. Lett.* **100**, 111602 (2012).
- ²⁰J. V. Goicochea, M. Hu, B. Michel, and D. Poulikakos, *J. Heat Transfer* **133**, 082401 (2011).
- ²¹Z. Liang and H.-L. Tsai, *J. Phys.: Condens. Matter* **23**, 495303 (2011).
- ²²T. S. English, J. C. Duda, J. L. Smoyer, D. A. Jordan, P. M. Norris, and L. V. Zhigilei, *Phys. Rev. B* **85**, 035438 (2012).
- ²³M. Hu, P. Keblinski, and P. K. Schelling, *Phys. Rev. B* **79**, 104305 (2009).
- ²⁴L. Hu, L. Zhang, M. Hu, J.-S. Wang, B. Li, and P. Keblinski, *Phys. Rev. B* **81**, 235427 (2010).
- ²⁵K. C. Collins, S. Chen, and G. Chen, *Appl. Phys. Lett.* **97**, 083102 (2010).
- ²⁶Z.-Y. Ong and E. Pop, *Phys. Rev. B* **81**, 155408 (2010).
- ²⁷Y. Wang and P. Keblinski, *Appl. Phys. Lett.* **99**, 073112 (2011).
- ²⁸J. C. Duda, T. S. English, E. S. Piekos, W. A. Soffa, L. V. Zhigilei, and P. E. Hopkins, *Phys. Rev. B* **84**, 193301 (2011).
- ²⁹M. Shen, W. J. Evans, D. Cahill, and P. Keblinski, *Phys. Rev. B* **84**, 195432 (2011).
- ³⁰P. E. Hopkins, M. Baraket, E. V. Barnat, T. E. Beechem, S. P. Kearney, J. C. Duda, J. T. Robinson, and S. G. Walton, *Nano Lett.* **12**, 590 (2012).
- ³¹R. Prasher, *Phys. Rev. B* **77**, 075424 (2008).
- ³²J. C. Duda, J. L. Smoyer, P. M. Norris, and P. E. Hopkins, *Appl. Phys. Lett.* **95**, 031912 (2009).
- ³³P. E. Hopkins, T. Beechem, J. C. Duda, K. Hattar, J. F. Ihlefeld, M. A. Rodriguez, and E. S. Piekos, *Phys. Rev. B* **84**, 125408 (2011).
- ³⁴J. Hirotsu, T. Ikuta, T. Nishiyama, and K. Takahashi, *Nanotechnology* **22**, 315702 (2011).
- ³⁵J. C. Duda, C. J. Kimmer, W. A. Soffa, R. E. Jones, and P. E. Hopkins, "Influence of crystallographic orientation and anisotropy on Kapitza conductance via classical molecular dynamics simulations," *J. Appl. Phys.* (unpublished).
- ³⁶P. G. Klemens, *Proc. Phys. Soc. London, Sec. A* **68**, 1113 (1955).
- ³⁷J. M. Ziman, *Electrons and Phonons*, 2nd ed. (Oxford University Press, New York, 1960).
- ³⁸A. Skye and P. K. Schelling, *J. Appl. Phys.* **103**, 113524 (2008).
- ³⁹D. V. Matyushov and R. Schmid, *J. Chem. Phys.* **104**, 8627 (1996).
- ⁴⁰M. P. Allen and D. J. Tildesley, *Computer Simulation of Liquids* (Clarendon, Oxford, 1990).
- ⁴¹H. J. C. Berendsen, J. P. M. Postma, W. F. van Gunsteren, A. DiNola, and J. R. Haak, *J. Chem. Phys.* **81**, 3684 (1984).
- ⁴²D. S. Ivanov and L. V. Zhigilei, *Phys. Rev. B* **68**, 064114 (2003).
- ⁴³J. C. Duda, T. S. English, D. A. Jordan, P. M. Norris, and W. A. Soffa, *J. Phys.: Condens. Matter* **23**, 205401 (2011).
- ⁴⁴D. G. Cahill, F. Watanabe, A. Rockett, and C. B. Vining, *Phys. Rev. B* **71**, 235202 (2005).
- ⁴⁵R. Cheaito, J. C. Duda, T. E. Beechem, K. Hattar, J. F. Ihlefeld, D. L. Medlin, M. A. Rodriguez, M. J. Champion, E. S. Piekos, and P. E. Hopkins, "Size effects on the thermal conductivity of silicon-germanium alloy thin films," *Phys. Rev. Lett.* (unpublished).